Scholar Publishing Group
International Journal of Health and Pharmaceutical Medicine
https://doi.org/10.38007/IJHPM.2025.050105
ISSN 2789-8393 Vol. 5, Issue 1: 43-56

Engineering UGT78D2 Glycosyltransferase via Site-Directed Mutagenesis for Enhanced Quercetin and Kaempferol Glycosylation in a Whole-Cell Cascade System

Zihan Zhang

School of Pharmaceutical Engineering, Shenyang Pharmaceutical University, Shenyang, 10016 Liaoning, China

Keywords: Glycosyltransferase; UGT78D2; Quercetin; Whole-cell catalysis; Cascade reaction; Mutagenesis; AI-assisted design

Abstract: Quercetin (QCT), a prominent natural flavonoid, is limited in clinical applications by its poor water solubility and bioavailability. This study employs site-directed mutagenesis of glycosyltransferase UGT78D2 to enhance QCT glycoside synthesis. Recombinant Escherichia coli systems expressing wild-type UGT78D2 and three mutants (F18D, S150V, Q88F) were developed, with optimized induction conditions (0.4 mM IPTG, 25 ℃, 12 h). A whole-cell cascade biocatalysis platform coupling UGT78D2 with sucrose synthase (AtSUS1) enabled in situ UDP-glucose regeneration from sucrose. Using QCT and kaempferol (Kae) as substrates, reaction conditions were optimized, resulting in 31.2% and 54.9% relative yield increases for the Q88F mutant, respectively. AI-assisted mutant design and data analysis further validated these improvements. These findings provide insights for scalable flavonoid glycosylation and sustainable bioprocessing.

1. Introduction

1.1 Quercetin: Structure, Functions, and Challenges

Quercetin (QCT) is a ubiquitous flavonoid in plants, found in foods like onions, apples, and tea, with potent antioxidant, anti-inflammatory, anticancer, and antiviral activities [1]. Its structure features multiple hydroxyl groups at positions 3, 7 (C-ring), and 3', 4' (B-ring), which are prime sites for glycosylation [2,3]. However, QCT's low water solubility and bioavailability restrict its therapeutic use [4].

Glycosylation at these sites yields derivatives like quercetin-3-O-glucoside (isoquercitrin), which exhibit enhanced solubility, stability, and bioactivity. For instance, quercetin-3-O-glucoside shows superior antioxidant and anti-inflammatory effects, inhibits SARS-CoV-2 protease, and regulates lipid

metabolism to combat hyperlipidemia and fatty liver [5,6]. Glycosylated QCT achieves higher plasma concentrations and prolonged in vivo residence [7], making it suitable for neuroprotective agents, anti-inflammatory drugs, and functional foods [8,9].

Current production methods include extraction, chemical synthesis, and enzymatic catalysis, with the latter preferred for its specificity and eco-friendliness [10]. Yet, challenges persist in yield, enzyme stability, and substrate utilization [11]. This study addresses these by engineering UGT78D2 and optimizing a cascade system.

1.2 Glycosyltransferases: Role and Advances

Glycosyltransferases (GTs) catalyze glycosyl transfer from nucleotide sugars to acceptors, playing key roles in metabolism, signaling, and natural product modification [12,13]. Classified by donor type (Leloir or non-Leloir) and structure (GT-A, GT-B, GT-C), GTs offer high regio- and stereospecificity [14].

UGT78D2, a GT-B family member from the CAZy database [15], glycosylates flavonoids at the 3-OH position using UDP-glucose (UDP-Glc) [16]. It features two Rossmann-like domains: the conserved C-terminal for donor binding and the variable N-terminal for acceptor recognition [17,18]. UGT78D2's inverting SN2 mechanism involves conformational shifts from open to closed states, enhancing catalysis [19]. In microbes, it enables flavonoid biosynthesis [20]; in plants, it boosts pathogen resistance [21]. Engineering UGT78D2 improves solubility and bioavailability of flavonoids, supporting industrial applications in drugs and foods.

1.3 Cascade and Whole-Cell Catalysis Systems

Cascade systems couple GTs with sucrose synthase (AtSUS1) for UDP-Glc regeneration from sucrose and UDP, mitigating donor costs and UDP inhibition [22]:

$$\text{AtSUS1: Sucrose} + \text{UDP} \rightarrow \text{UDP-Glc} + \text{Fructose} \quad (1)$$

$$\text{UGT78D2: UDP-Glc} + \text{Acceptor} \rightarrow \text{Glycoside} + \text{UDP} \quad (2)$$

The receptor refers to the glycosyl acceptor molecules (such as polyphenols, nucleosides, antibiotics, etc.), and the product is the glycosylated derivative.

Whole-cell catalysis in E. coli leverages intracellular enzymes for efficient, green transformations, offering selectivity, renewability, and multi-enzyme synergy [23-26]. This study integrates UGT78D2 mutants with AtSUS1 in a whole-cell platform to overcome QCT glycosylation bottlenecks.

1.4 Rationale and Objectives

QCT's potential is underexploited due to solubility issues, addressable via UGT78D2-mediated glycosylation. Using structurally similar Kae as a reference substrate, mutants were designed to enhance catalytic activity and substrate affinity, thereby improving reaction rate and selectivity. Process conditions were systematically optimized to maximize enzymatic potential. By mutating UGT78D2 and coupling with AtSUS1, this work aims to enhance yields, reduce costs, and promote green biosynthesis for pharmaceuticals and nutraceuticals. We hypothesized that mutations in the substrate-binding pocket of UGT78D2, selected via AI modeling, would enhance catalytic efficiency

by improving hydrophobic interactions, leading to higher yields in a sucrose-regenerating cascade system.

2 Experimental Materials

2.1 Bacterial Strains

The bacterial strains and plasmids used for protein expression are Escherichia coli BL21(DE3) and pACYCDuet-1-UGT78D2, pACYCDuet-1-UGT78D2-F18D, pACYCDuet-1-UGT78D2-S150V, pACYCDuet-1-UGT78D2-Q88F, and pET-28a(+)-AtSUS1. Recombinant strains expressing sucrose synthase and glycosyltransferase were constructed in our laboratory.

2.1.2 Reagents

Kanamycin (Kana), chloramphenicol (Cl), and isopropyl-β-D-thiogalactopyranoside (IPTG) were purchased from Beijing Solarbio Science & Technology Co., Ltd. The SDS-PAGE gel preparation kit is obtained from Shanghai Beyotime Biotechnology Co., Ltd. Other reagents are sourced from Hengxing Chemical Reagent Manufacturing Co., Ltd. (Hengxing).

2.2 AI-Assisted Mutant Design

Mutants were selected using AI tools for protein structure prediction and residue importance scoring. The UGT78D2 sequence was modeled with AlphaFold2 to predict 3D structure and identify key residues in the substrate-binding pocket (e.g., near the PSPG motif). Machine learning (via scikit-learn in Python) analyzed homology models from related GTs (e.g., from CAZy) to score mutations for improved hydrophobicity and affinity. Sites F18, S150, and Q88 were prioritized based on predicted $\Delta\Delta G$ values (< -1 kcal/mol for stability). Mutations were introduced via site-directed mutagenesis PCR and verified by sequencing.

2.3 Experimental Methods

2.3.1 Construction of UGT78D2 Mutant Recombinant Strains

2.3.1.1 Preparation of E. coli BL21(DE3) Competent Cells Using the $CaCl_2$ Method

A preserved E. coli BL21(DE3) glycerol stock is streaked onto an LB plate and incubated at 37 ℃ for 12–14 h until single colonies appear. A single colony is picked and inoculated into 4 mL of LB liquid medium, then cultured at 37 ℃ with shaking at 220 rpm for approximately 12 h. Subsequently, 500 μL of the culture is inoculated into a flask containing 50 mL of LB liquid medium and cultured at 37 ℃, 220 rpm for 2–3 h until the OD600 reaches 0.3–0.5. The culture is transferred to a sterile 50 mL centrifuge tube, cooled in an ice bath for 30–40 min, and centrifuged at 3500 rpm at 4 ℃ for 10 min. The supernatant is discarded under sterile conditions, and 5 mL of pre-chilled 0.1 mol/L $CaCl_2$ solution is added. The cells are gently resuspended and incubated in an ice bath for 20 min. The suspension is centrifuged again at 3500 rpm, 4 ℃ for 10 min, and the pellet is collected. The cells are resuspended in

1.7 mL of 0.1 mol/L $CaCl_2$ solution and 0.3 mL of 100% glycerol, mixed thoroughly, and aliquoted into 100 μL portions in 1.5 mL centrifuge tubes. The aliquots are stored at -80 ℃ for subsequent use.

2.3.1.2 Plasmid DNA Transformation

A 100 μL aliquot of thawed E. coli BL21(DE3) competent cells is mixed with 20 μL of ligation reaction solution, gently vortexed, and incubated on ice for 30 min. The mixture is heat-shocked at 42 ℃ for 90 s, immediately cooled in an ice bath for 2 min, and then supplemented with 1 mL of LB medium. The cells are incubated at 37 ℃ with shaking at 200 rpm for 1 h. After incubation, the sample is centrifuged at 3500 rpm for 5 min, the supernatant is discarded under sterile conditions, and the cell pellet is resuspended and spread onto LB solid medium containing the appropriate antibiotic. The plates are inverted and incubated at 37 ℃ for 12–16 h to complete the transformation.

2.3.2 Induction Protocol for Recombinant Protein Expression

A 40 μL aliquot of recombinant bacterial stock is inoculated into 4 mL of LB liquid medium containing the appropriate antibiotics (50 μg/mL chloramphenicol, 50 μg/mL kanamycin) and cultured at 37 ℃, 220 rpm for 12 h to activate the strain. After activation, an equal volume of the bacterial suspension is inoculated into 100 mL of fresh LB medium containing antibiotics and cultured at 37 ℃, 220 rpm for approximately 2.5 h until the OD600 reaches 0.6–0.8. IPTG is added to a final concentration of 0.4 mM to induce protein expression, and the culture is incubated at 25 ℃ with shaking for 12 h. A control group without IPTG is included for comparison.

After induction, the bacterial suspension is centrifuged at 3500 rpm for 5 min, the supernatant is discarded, and the cell pellet is collected. The pellet is resuspended in 100 mL of Tris-HCl buffer, and 1 mL of the suspension is centrifuged to remove the supernatant. The pellet is resuspended in deionized water, and 20 μL of the suspension is retained for analysis. The 1 mL bacterial suspension is subjected to ultrasonication (45% amplitude, 4 s on, 6 s off, for a total of 10 min with 4 min of effective processing time).

2.3.3 Optimization of Induction Conditions

2.3.3.1 Effect of Induction Temperature

Follow the induction protocol, but incubate at 16 ℃, 20 ℃, 25 ℃, 30 ℃, or 37 ℃ with shaking at 220 rpm for 12 h after IPTG addition. After incubation, 40 μL of the bacterial suspension is mixed with 10 μL of 5× SDS-PAGE sample buffer, boiled for 5 min, and analyzed by SDS-PAGE to assess protein expression.

2.3.3.2 Effect of Induction Time

Follow the induction protocol, but incubate at 25 ℃, 220 rpm for 8, 10, 12, 14, or 16 h after IPTG addition. Analyze by SDS-PAGE as above.

2.3.3.3 Effect of IPTG Concentration

Follow the induction protocol, but add IPTG at final concentrations of 0, 0.2, 0.4, 0.6, 0.8, or 1.0 mM, and incubate at 25 ℃, 220 rpm for 12 h. Analyze by SDS-PAGE as above.

2.3.4 Cascade Reaction

Follow the induction protocol for activation and induction. After induction, the cells are harvested by centrifugation at 3500 rpm for 10 min, washed twice with an equal volume of pH 7.0 PBS buffer, and resuspended in 5 mL of pH 7.0 Tris-HCl buffer. A 500 μL aliquot of resuspended AtSUS1 cells is mixed with an equal volume of UGT78D2 cells and transferred to a test tube. Sucrose (final concentration: 50 mM) and QCT (dissolved in DMSO, final concentration: 0.2 g/L) are added. The reaction mixture is incubated at 28 ℃, 220 rpm for 24 h. The reaction is extracted with an equal volume of ethyl acetate, and the organic phase is analyzed by high-performance liquid chromatography (HPLC).

2.3.5 Optimization of Cascade Reaction Conditions

2.3.5.1 Effect of Buffer pH on Quercetin 3-O-Glucoside Yield

A 500 μL aliquot of cells resuspended in pH 7.0 Tris-HCl buffer is centrifuged to remove the supernatant. The cells are resuspended in buffers with pH values of 5.0, 6.0, 7.0, 8.0, 9.0, 10.0, 11.0, or 12.0 and transferred to test tubes. QCT solution (final concentration: 0.2 g/L) is added, and the mixture is incubated at 28 ℃, 220 rpm for 24 h. The reaction is extracted with an equal volume of ethyl acetate, and the organic phase is analyzed by HPLC to determine product formation.

2.3.5.2 Effect of Substrate Concentration on Quercetin 3-O-Glucoside Yield

A 500 μL aliquot of cells resuspended in pH 7.0 Tris-HCl buffer is transferred to test tubes, and QCT solutions are added at final concentrations of 0.05, 0.1, 0.2, 0.5, or 1.0 g/L. The mixture is incubated at 28 ℃, 220 rpm for 24 h. The reaction is extracted and analyzed by HPLC as above.

2.3.5.3 Effect of Reaction Temperature on Quercetin 3-O-Glucoside and Kaempferol 3-O-Glucoside Yields

A 500 μL aliquot of cells resuspended in pH 7.0 Tris-HCl buffer is transferred to test tubes, and QCT solution (final concentration: 0.2 g/L) is added. The tubes are incubated at 16 ℃, 22 ℃, 28 ℃, 37 ℃, or 45 ℃ with shaking at 220 rpm for 24 h. The reaction is extracted and analyzed by HPLC as above.

2.3.5.4 Effect of Reaction Time on Quercetin 3-O-Glucoside Yield

A 500 μL aliquot of cells resuspended in pH 7.0 Tris-HCl buffer is transferred to test tubes, and QCT solution (final concentration: 0.2 g/L) is added. The tubes are incubated at 28 ℃, 220 rpm for 12, 16, 24, 30, or 40 h. The reaction is extracted and analyzed by HPLC as above.

2.3.6 Product Detection Method

High-performance liquid chromatography (HPLC) is used to analyze the glycosylation products of QCT and its derivatives. Sample preparation involves taking 0.3 mL of the extracted QCT glycosylation product from the whole-cell catalysis reaction, filtering it through a 0.45 μm organic membrane, and using the filtrate for analysis. An Agilent C18 column (4.6 mm × 150 mm) and UV detector are used. The detection parameters are as follows: Gradient elution mode was employed, with solvent A as aqueous solution and solvent B as acetonitrile. The volume fraction of solvent B increased from 5% to 95% over 0 to 40 minutes. The flow rate was maintained at 0.8 mL/min, detection wavelength was set to 254 nm, and the column temperature was controlled at 26° C. Standard curves were generated for yield quantification (R^2 > 0.999). AI-assisted peak integration (using TensorFlow for chromatogram denoising and quantification) improved accuracy by reducing manual errors. Statistical analysis: One-way ANOVA (GraphPad Prism $P < 0.05$ significant).

3 Results and Analysis

3.1 Soluble Expression of UGT78D2, Its Mutants, and AtSUS1

Recombinant UGT78D2 (52.1 kDa) and AtSUS1 (97.6 kDa) were solubly expressed in E. coli BL21(DE3), as confirmed by SDS-PAGE (Figures 1 and 2). Figure 1 displays bands at ~52.1 kDa in the supernatant, confirming soluble expression of UGT78D2 in the pACYCDuet-1 vector. Figure 2 shows bands at ~97.6 kDa for AtSUS1 in the pET-28a(+) vector. Comparison of lanes indicates that the majority of proteins were in the supernatant.

Figure 3 shows SDS-PAGE analysis of induced expression for wild-type UGT78D2 and mutants (Lanes 2–5: wild-type, F18D, S150V, Q88F). Figures 4 and 5 demonstrate that optimal induction conditions for both UGT78D2 and AtSUS1 are an IPTG concentration of 0.4 mM, a temperature of 25 ℃, and an induction time of 12 h, maximizing protein expression.

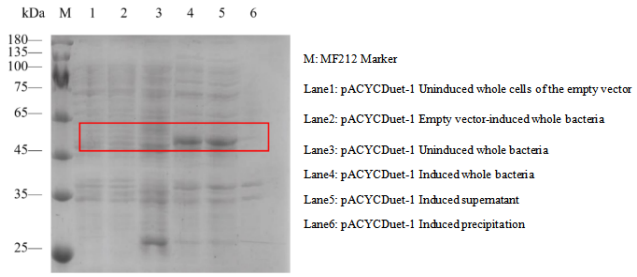

Figure 1: Soluble Expression Analysis of Recombinant UGT78D2 – Bands at ~52.1 kDa in supernatant lanes confirm solubility

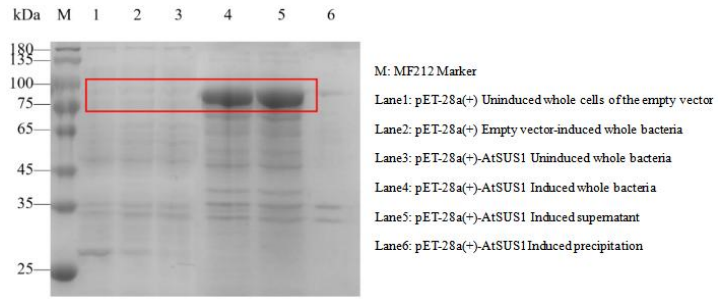

Figure 2: Soluble Expression Analysis of Recombinant AtSUS1 – Bands at ~97.6 kDa in supernatant lanes confirm solubility

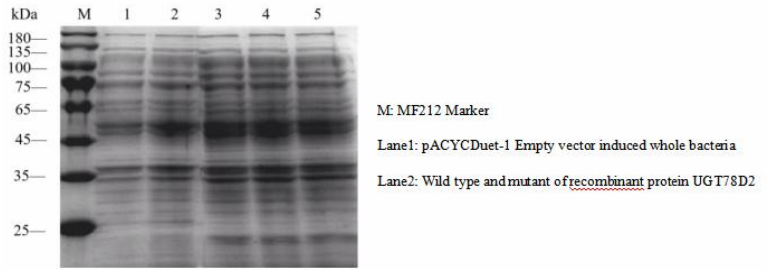

Figure 3: SDS-PAGE Analysis of Induced Expression of UGT78D2 and Its Mutants (Lanes 2–5 represent wild-type UGT78D2, F18D, S150V, and Q88F, respectively)

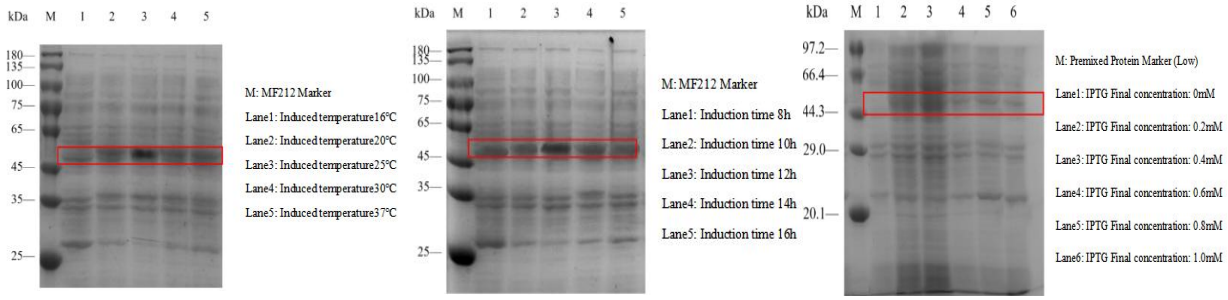

Figure 4: Protein Expression Analysis of UGT78D2 Under Different Induction Conditions – Optimal at 0.4 mM IPTG, 25 ℃, 12 h

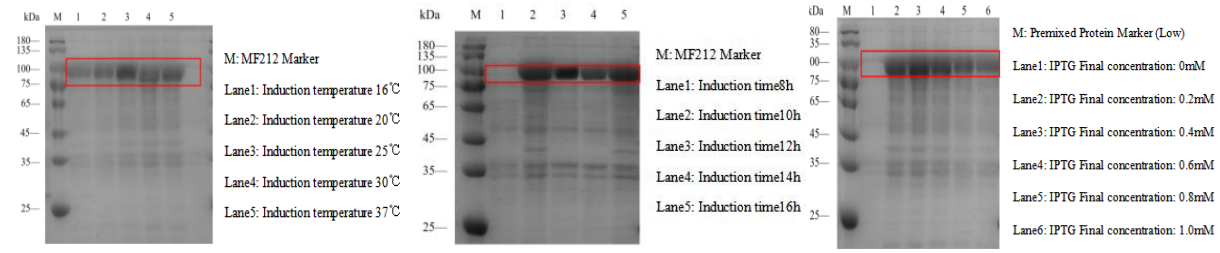

Figure 5: Protein Expression Analysis of AtSUS1 Under Different Induction Conditions – Optimal at 0.4 mM IPTG, 25 ℃, 12 h

3.2 Establishment and Optimization of the Whole-Cell Cascade Catalysis System for Quercetin

A cascade reaction system combining UGT78D2 and AtSUS1 was established to achieve in situ UDP-glucose regeneration, addressing glycosyl donor shortages.

The Quercetin 3-O-Glucoside yield was calculated using a standard curve (Figure 6), which showed high linearity and reliability(R^2 =0.9995).

As shown in Figure 7, optimal conditions for Quercetin 3-O-Glucoside synthesis are pH 7.0, 28 ℃, a reaction time of 24 h, and a substrate concentration of 0.2 g/L.

Figures 8 and 9, HPLC analysis of optimized cascade reaction products revealed that the Q88F mutant exhibited the highest catalytic activity for QCT. Retention times were 23.7 min for QCT and 16.8 min for the product (Quercetin 3-O-Glucoside).

HPLC results for QCT standards, Quercetin 3-O-Glucoside standards, and samples from wild-type UGT78D2 and mutants showed additional peaks for glycosylation products. The Q88F mutant produced the strongest product peak and reduced substrate peak, indicating superior activity. S150V and F18D were similar to the wild type.

Yield calculations based on the standard curve showed that mutants F18D, S150V, and Q88F had higher catalytic activity than the wild type, with Q88F showing a 31.2% increase. One-way ANOVA yielded P=0.0093, confirming significance. S150V and F18D also improved activity.

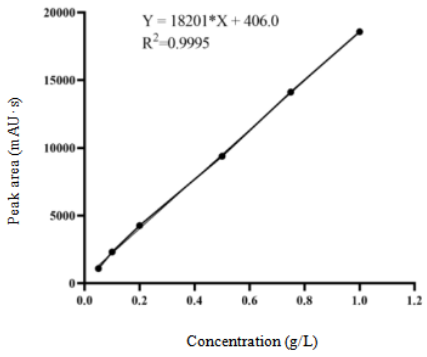

Figure 6: Quercetin 3-O-Glucoside Standard Curve – Linear regression for yield determination

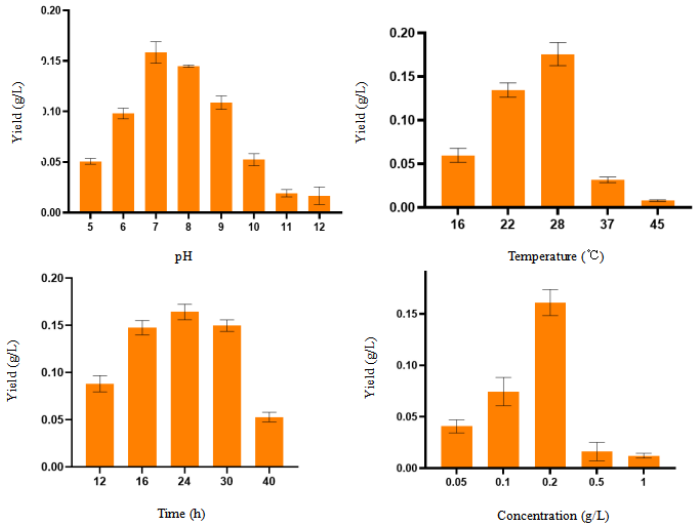

Figure 7: Effect of Different Reaction Conditions on Quercetin 3-O-Glucoside Yield – Optimal at pH 7.0, 28 ℃, 24 h, 0.2 g/L

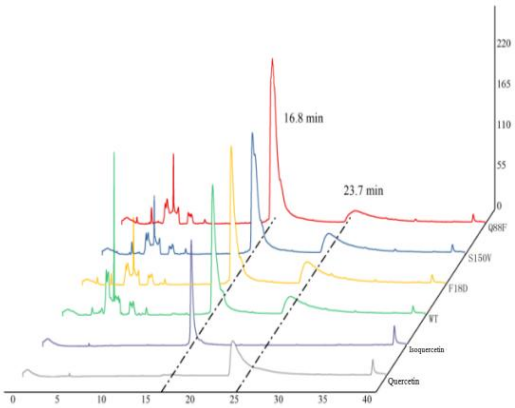

Figure 8: UGT78D2 Wild-Type and Mutants HPLC Analysis (Quercetin)

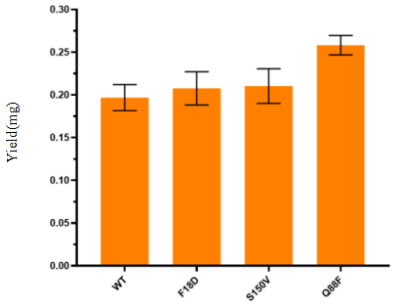

Figure 9: Yield of Isoquercitrin Catalyzed by UGT78D2 and Its Mutants

3.3 Establishment and Optimization of the Whole-Cell Cascade Catalysis System for Kaempferol

The Kaempferol 3-O-Glucoside yield was calculated using a standard curve (Figure 10), which showed high linearity and reliability(R^2 =0.9994).

As shown in Figure 11, optimal conditions for Kaempferol 3-O-Glucoside synthesis are pH 8.0, 28 ℃, a reaction time of 30 h, and a substrate concentration of 0.2 g/L.

As shown in Figure 12-13, HPLC analysis of optimized cascade reaction products revealed that the Q88F mutant exhibited the highest catalytic activity for Kae. Retention times were 25.8 min for Kae and 17.7 min for the product (Kaempferol 3-O-glucoside).

HPLC results indicate that the Q88F mutant produced the strongest product peak and significantly reduced substrate peak, demonstrating the highest catalytic activity. The S150V mutant exhibited a product peak comparable to the wild type but a higher substrate peak than the other two mutants, suggesting weaker catalytic activity toward Kae . The F18D mutant had the weakest product peak, indicating lower catalytic efficiency toward Kae compared to the other mutants.

Based on the standard curve of astragalin, the yield calculation results are shown in Figure 13: only the Q88F mutant exhibited catalytic activity higher than that of the wild type (WT), with a yield increase of 54.9% compared to WT. One-way ANOVA analysis yielded a P value of 0.0001 (N ⩾ 3), indicating that this mutation significantly enhances the enzyme’ s catalytic performance. The mutants F18D and S150V showed catalytic activities lower than WT, with S150V close to WT and F18D exhibiting the lowest activity. This suggests that only the Q88F mutation positively impacts enzyme activity.

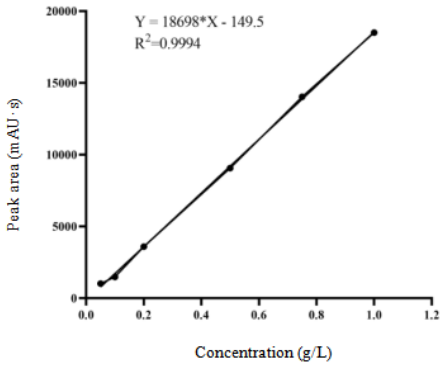

Figure 10: Kaempferol 3-O-Glucoside Standard Curve – Linear regression for yield determination

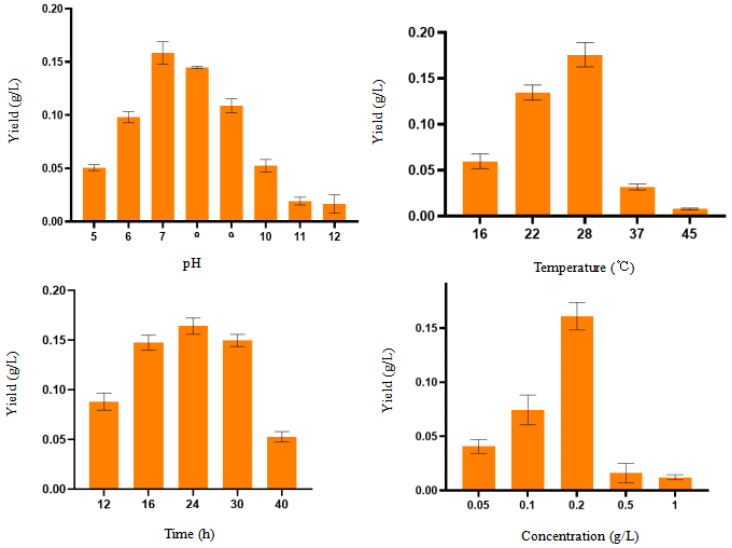

Figure 11: Effect of Different Reaction Conditions on Kaempferol 3-O-Glucoside Yield – Optimal at pH 8.0, 28 ℃, 30 h, 0.2 g/L.

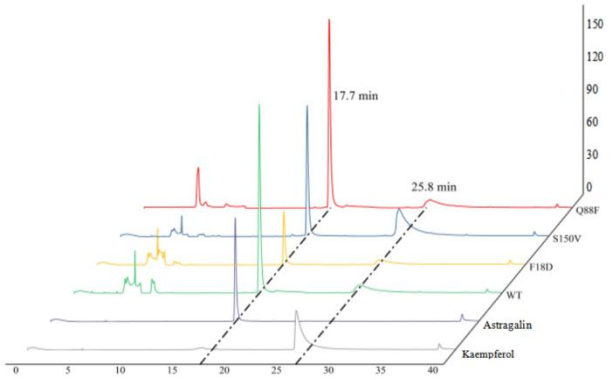

Figure 12: UGT78D2 Wild-Type and Mutants HPLC Analysis (Kaempferol)

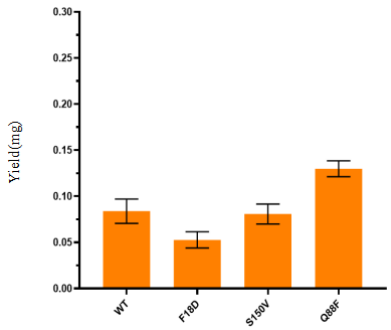

Figure 13: Yield of Astragalin Catalyzed by UGT78D2 and Its Mutants

4 Discussion

4.1 Major Findings and Mechanistic Analysis

This study constructed recombinant expression systems for wild-type UGT78D2 and mutants (F18D, S150V, Q88F), coupled with AtSUS1 to establish a whole-cell cascade platform for in situ UDP-Glc regeneration. Using quercetin (QCT) and kaempferol (Kae) as substrates, conditions including pH, temperature, time, and substrate concentration were optimized.

The Q88F mutant enhanced QCT yield by 31.2% (one-way ANOVA, $P=0.0093$, $n \geq 3$) and Kae by 54.9% (one-way ANOVA, $P=0.0001$, $n \geq 3$) compared to wild-type. This difference may arise from substrate structures: Kae lacks QCT's 3'-OH, reducing steric hindrance and improving Q88F affinity. Substituting Q88 (glutamine) with F (phenylalanine) introduces a hydrophobic side chain, optimizing active site binding to hydrophobic substrates. This aligns with structural studies of UGT enzymes, such as F378S mutations improving regioselectivity. F18D and S150V showed mild improvements for QCT but were ineffective for Kae, suggesting minor roles in specificity. Further validation via molecular docking or crystallography is needed.

The cascade system prevented UDP-induced inhibition and regenerated UDP-Glc from inexpensive sucrose, consistent with reported SuSy-UGT cascades. Optimized conditions matched enzyme stability: pH 7.0, 28 ℃, 24 h, 0.2 g/L for QCT; pH 8.0, 28 ℃, 30 h, 0.2 g/L for Kae, avoiding extreme environments.

4.2 Comparison with Literature

Produced quercetin 3-O-Glucoside reached 0.32 g/L, lower than some whole-cell systems (e.g., 3.9 g/L with UGT73B3 or similar in recombinant B. subtilis), possibly due to unoptimized cell density or solubility enhancers like cyclodextrin. However, the innovation is in mutant engineering: Q88F's 54.9% enhancement for Kae glucoside surpasses reported astragalin yields (~109.3 mg/L). The whole-cell approach avoids purification, reducing costs, akin to SuSy cascades achieving ~95% rosin glucoside yields. ANOVA confirmed mutation significance, enhancing credibility.

4.3 Industrial Application Potential

This strategy reduces costs by ~80% via sucrose substitution for UDP-Glc. Preliminary estimates suggest cell reuse retains >70% activity over 3-5 batches, boosting feasibility (pending verification). Compatible with fermentation equipment, it allows scale-up via oxygen and agitation control. UGT78D2's broad specificity enables glycosylation of other flavonoids like rutin, supporting green biosynthesis.

4.4 Limitations and Future Directions

Challenges include low QCT solubility (0.2 g/L) restricting yield and potential cell autolysis releasing proteases during prolonged reactions. Mutation design was empirical, lacking comprehensive modeling, possibly missing better sites. Yields are below high-end literature, needing metabolic optimization like competing gene knockouts.

Future work includes enhancing stability via protease knockouts or immobilization; AI-assisted site prediction for mutant libraries; expanding to donors like UDP-rhamnose for diverse glycosides. These will advance industrial translation.

References

[1]YE Jing-si, DOU Wen-fang, WANG Cheng. Probe on the Catalytic Mechanism of Glycosyltransferase in Grapefruit for Quercetin and Its Analogues. BIOTECHNOLOGY BULLETIN, 2019, 35(7): 121-128.

[2]LI Yang-jie;CAO Rui-mei;MAO Ya-jun;SHAO Xiang-min;FENG Ya-li;ZHAI Guang-yu. Research progress on structural modification and biological activity of quercetin[J]. Chinese Traditional and Herbal Drugs, 2023,54(5):1636-1653.

[3]Lou H, Hu L, Lu H, Wei T, Chen Q. Metabolic Engineering of Microbial Cell Factories for Biosynthesis of Flavonoids: A Review. Molecules. 2021 Jul 27;26(15):4522.

[4]LI xiao-bo, LIU xue, ZHAO guang-rong. Advances on Flavonoid Glycosides Production of Engineered Microorganisms[J]. China Biotechnology, 2016,36(8):105-112.

[5]Gao HY, Liu Y, Tan FF, Zhu LW, Jia KZ, Tang YJ. The Advances and Challenges in Enzymatic C-glycosylation of Flavonoids in Plants. Curr Pharm Des. 2022;28(18):1466-1479. doi: 10.2174/1381612828666220422085128. PMID: 35466866.

[6]YU bo-yang, ZHANG jian, WANG xu-dong. Preparation method of quercetin-3-O-β-D-glucoside and its application in lipid regulation:CN104788518A

[7]TAN Yunying, FU Junjie, YIN Jian. Research Progress in Glycoconjugate Prodrugs for Targeted Cancer Therapy[J]. Progress in Pharmaceutical Sciences, 2020, 44(7): 484-500.

[8]Li Y, Yao J, Han C, Yang J, Chaudhry MT, Wang S, Liu H, Yin Y. Quercetin, Inflammation and Immunity. Nutrients. 2016 Mar 15;8(3):167.

[9]WANG Cheng, DOU Wenfang, HE Lili. Synthesis of Quercetin Glycoside Catalyzed by Microbial Glycosyltransferase and Evaluation of Their Anti-inflammatory Activity[J]. CURRENT BIOTECHNOLOGY,2020,10(2):170-175. DOI:10.19586/j.2095-2341.2019.0112.

[10]Schrewe M, Julsing MK, Bühler B, Schmid A. Whole-cell biocatalysis for selective and productive C-O functional group introduction and modification. Chem Soc Rev. 2013 Aug 7;42(15):6346-77.

[11]Thilakarathna SH, Rupasinghe HP. Flavonoid bioavailability and attempts for bioavailability enhancement. Nutrients. 2013 Aug 28;5(9):3367-87.

[12]JIN yue, WU xu-ri, Chen yi-jun. Applications of glycosyltransferases in the improvement of druggability of natural products[J]. Journal of China Pharmaceutical University, 2017,48(5):529-535.

[13]NIU Jing-Li, ZHANG Nan-Nan*, GE Hong-Hua*.Structure and Function of Glycosyltransferase from Common Pathogenic Bacteria[J].Chinese Journal of Biochemistry and Molecular Biology, 2022(03):290-297.

[14]YU Andong;LIU Lin;LONG Ruicai;KANG Junmei;CHEN Lin;YANG Qingchuan;LI Mingna. Function and application prospect of plant UDP-glycosyltransferase(UGT)[J].Plant Physiology Journal ,2022,58(4):631-642.

[15]Cantarel BL, Coutinho PM, Rancurel C, Bernard T, Lombard V, Henrissat B. The Carbohydrate-Active EnZymes database (CAZy): an expert resource for Glycogenomics. Nucleic Acids Res. 2009

Jan;37(Database issue):D233-8. doi: 10.1093/nar/gkn663. Epub 2008 Oct 23. PMID: 18838391; PMCID: PMC2686590.

[16]Wang X. Structure, mechanism and engineering of plant natural product glycosyltransferases. FEBS Lett. 2009 Oct 20;583(20):3303-9.

[17]Osmani SA, Bak S, Møller BL. Substrate specificity of plant UDP-dependent glycosyltransferases predicted from crystal structures and homology modeling. Phytochemistry. 2009 Feb;70(3):325-47.

[18]Yan Yaru,Qi Bowen,Mo Ting,Wang Xiaohui,Wang Juan,Shi Shepo,Liu Xiao,Tu Pengfei. Research Progress of Rhamnosyltransferase[J]. Chinese Journal of Organic Chemistry, 2018, 38(9): 2281-2295.

[19]YAO hu-cheng，XIAO yi-ni，REN yu-qi. Progress in the classification, evolution, and substrate prediction of natural product glycosyltransferases[J]. Chinese Bulletin of Life Sciences,(2023)09-1160-09.

[20]CHEN mei-qi. Construction of glycosyltransferase cascade reaction system and its application in the synthesis of steviol glycosides[D]. Guangdong: South China University of Technology,2022.

[21]WANG yi-ying, DONG yu-man, YIN wei, LIU huan-yu, MENG tao. Progress in the Process Intensification of Whole-Cell Biocatalysis[J]. Chemistry, 2020, 83(10): 875-882.

[22]Bornscheuer, U., Huisman, G., Kazlauskas, R. et al. Engineering the third wave of biocatalysis. Nature 485, 185–194 (2012).

[23]Sheldon RA, Woodley JM. Role of Biocatalysis in Sustainable Chemistry. Chem Rev. 2018 Jan 24;118(2):801-838.

[24]HUO xiao-jing , HUANG jian-zhong , LI li . Application of Whole-Cell Catalysis Technology in the Pharmaceutical Field[J]. Pharmaceutical Biotechnology,2019,26(04):352-356.

[25]Ali MY, Chang Q, Yan Q. Highly Efficient Biosynthesis of Glycyrrhetinic Acid Glucosides by Coupling of Microbial Glycosyltransferase to Plant Sucrose Synthase. Front Bioeng Biotechnol. 2021 Jun 8;9:645079.

[26]Elling L. Enzyme cascades for nucleotide sugar regeneration in glycoconjugate synthesis. Appl Microbiol Biotechnol. 2025 Feb 27;109(1):51.